Robotica (1998) volume 16, pp. 615–621. Printed in the United Kingdom © 1998 Cambridge University Press

Computer simulation of robot dynamics

M. Eroglu

Department of Mechanical Engineering, Faculty of Engineering, Gazi University, 06570 Maltepe/ANKARA (Turkey)
e-mail: meroglu@mikasa.mmf.gazi.edu.tr

(Received in Final Form: February 14, 1998)

SUMMARY
This paper contains the result of a computer simulation of the dynamic performance of a manipulator. Provision is made in the program developed to represent the manipulator in either a redundant or non-redundant form. The models derived are used in simulation studies to evaluate the dynamic behaviour of the process when subjected to different control strategies for a range of operational tasks. The dynamic manipulator model presented is derived from the laws of Newtonian and Lagrangian Mechanics.

KEYWORDS: Computer simulation; Robot dynamics; Control strategies; Manipulator model.

1. MODEL FOR MANIPULATOR DYNAMICS

The general equation of motion for an open chain manipulator can be conveniently expressed through the application of Lagrangian equations. The Denavit-Hartenberg matrix representation can be utilized to describe the displacement between the neighbouring link coordinate frames to obtain the link kinematic information. The algorithm which describes the manipulator motion is the Lagrange Equation[1] which is normally written

$$\mathrm{T_i} = \frac{\partial}{\partial \mathrm{t}}\left[\frac{\partial \mathrm{L}}{\partial \dot{q}_i}\right] - \frac{\partial L}{\partial q_i} \qquad (1)$$

where L is known as Lagrangian and is the difference between the kinetic and potential energies of the manipulator. The Term $\mathrm{T_i}$ represents the torque generated by the ith actuator. The use of the Lagrange Equation will yield directly as many equations of motion as the number of degrees of freedom of the system when the basic energy expressions for the system are known. For a manipulator, the Lagrangian can be defined as[2–4]

$$L = \sum_{i=1}^{n}\sum_{j=1}^{i}\sum_{k=1}^{l} T_r(U_{ij}J_iU_{ik}^T)\dot{q}_i\dot{q}_k + \sum_{i=1}^{n} m_i g(T_i r_i) \qquad (2)$$

For $i = 1,2,\ldots,$n Equation 1 can be expressed as

$$T_{\mathrm{i}} = \sum_{k=1}^{n} D_{ik}\ddot{q}_k + \sum_{\mathrm{j}=1}^{\mathrm{n}}\sum_{\mathrm{k}=1}^{\mathrm{n}} \mathrm{h}_{ijk}\dot{q}_j\dot{q}_k + C_i \qquad (3)$$

and in a matrix form as

$$T = D(q)\ddot{q} + h(q,\dot{q}) + C(q) \qquad (4)$$

The remaining parameter contained within the first term of Equation 4 is J_i. Thus an inertia matrix which can be written as:-

$$J_i = \begin{matrix} \frac{-I_{xx}+I_{yy}+Izz}{2} & I_{xy} & I_{xz} & m_i\bar{x}_i \\ I_{xy} & \frac{-I_{xx}+I_{yy}+I_{zz}}{2} & I_{yz} & m_i\bar{y}_i \\ I_{xz} & I_{yz} & \frac{-I_{xx}+I_{yy}+I_{zz}}{2} & m_i\bar{z}_i \\ m_i\bar{x}_i & m_i\bar{y}_i & m_i y_i & m_i \end{matrix} \qquad (5)$$

and the elements of this matrix are the inertia tensor where the indices, x, y and z indicate the axes of the coordinate frame. The terms $\bar{x}$, $\bar{y}$ and $\bar{z}$ are the centre of mass vector of a link measured from the link coordinate frame.

2. DYNAMIC EQUATIONS FOR THE MANIPULATOR

The dynamic equations relate torque to position, velocity and acceleration and the solution of these equations allows the motions of the manipulator to be found. These dynamic equations are normally expressed in a matrix form in order to obtain the necessary information for control. The analysis of the dynamics and the design of an appropriate controller for the six-degree-of-freedom manipulator requires analytic expressions for the manipulator's dynamic coefficients previously defined. The dynbamic coefficients for a six DOF manipulator are complex and expressions become rapidly unmanageable unless assumptions are made about the dynamics of the manipulators.[5]

The restriction made in this study is that for dynamic analysis purposes joints 5 and 6 will be assumed fixed in Figure 1. These links will be kept in a known configuration, thus allowing for the derivation of relatively simple analytic expressions for the dynamic coefficients. If the algorithm given by Equation 3 is expanded in general terms for the non-redundant manipulator, the following equations of motion are obtained:

$$\begin{aligned} T_1 = {} & D_{11}\ddot{q}_1 + D_{12}\ddot{q}_2 + D_{13}\ddot{q}_3 + D_{14}\ddot{q}_4 + h_{111}\dot{q}_1^2 \\ & + h_{122}\dot{q}_2^2 + h_{133}\dot{q}_3^2 + h_{144}\dot{q}_4^2 + h_{112}\dot{q}_1\dot{q}_2 + h_{113}\dot{q}_1\dot{q}_3 \\ & + h_{114}\dot{q}_1\dot{q}_4 + h_{123}\dot{q}_2\dot{q}_3 + h_{124}\dot{q}_2\dot{q}_4 + h_{134}\dot{q}_3\dot{q}_4 + C_1 \end{aligned} \qquad (6)$$

$$\begin{aligned} \mathrm{T}_2 = {} & \mathrm{D}_{12}\ddot{\mathrm{q}}_1 + \mathrm{D}_{22}\ddot{\mathrm{q}}_2 + \mathrm{D}_{23}\ddot{\mathrm{q}}_3 + \mathrm{D}_{24}\ddot{\mathrm{q}}_4 + \mathrm{h}_{211}\dot{\mathrm{q}}_1^2 \\ & + \mathrm{h}_{222}\dot{\mathrm{q}}_2^2 + \mathrm{h}_{233}\dot{\mathrm{q}}_3^2 + \mathrm{h}_{244}\dot{\mathrm{q}}_4^2 + \mathrm{h}_{212}\dot{\mathrm{q}}_1\dot{\mathrm{q}}_2 + \mathrm{h}_{213}\dot{\mathrm{q}}_1\dot{\mathrm{q}}_3 \\ & + h_{214}\dot{q}_1\dot{q}_4 + h_{223}\dot{q}_2\dot{q}_3 + h_{224}\dot{q}_2\dot{q}_4 + h_{234}\dot{q}_3\dot{q}_4 + C_2 \end{aligned} \qquad (7)$$

https://doi.org/10.1017/S0263574798000617 Published online by Cambridge University Press

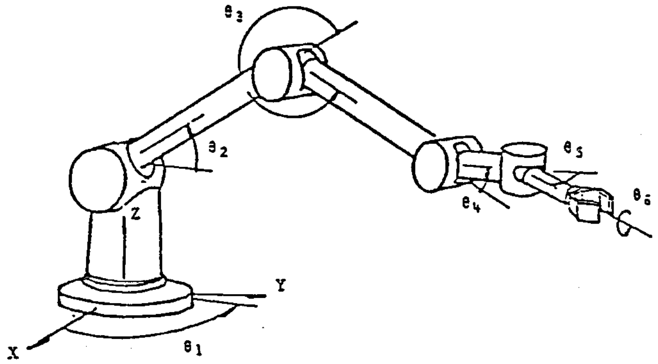

Fig. 1. Six Degree of manipulator

$$\mathrm{T}_3 = \mathrm{D}_{13}\ddot{\mathrm{q}}_1 + \mathrm{D}_{23}\ddot{\mathrm{q}}_2 + \mathrm{D}_{33}\ddot{\mathrm{q}}_3 + \mathrm{D}_{34}\ddot{\mathrm{q}}_4 + \mathrm{h}_{311}\ddot{\mathrm{q}}_1^2 + \mathrm{h}_{322}\dot{\mathrm{q}}_2^2 + \mathrm{h}_{333}\dot{\mathrm{q}}_4^2 + \mathrm{h}_{344}\dot{\mathrm{q}}_4^2 + \mathrm{h}_{312}\dot{\mathrm{q}}_1\dot{\mathrm{q}}_2 + \mathrm{h}_{313}\dot{\mathrm{q}}_1\dot{\mathrm{q}}_3 + h_{314}\dot{q}_1\dot{q}_4 + h_{323}\dot{q}_2\dot{q}_3 + h_{324}\dot{q}_2\dot{q}_4 + h_{334}\dot{q}_3\dot{q}_4 + C_3 \quad (8)$$

$$\mathrm{T}_3 = \mathrm{D}_{14}\ddot{\mathrm{q}}_1 + \mathrm{D}_{24}\ddot{\mathrm{q}}_2 + \mathrm{D}_{34}\ddot{\mathrm{q}}_3 + \mathrm{D}_{44}\ddot{\mathrm{q}}_4 + \mathrm{h}_{411}\ddot{\mathrm{q}}_1^2 + \mathrm{h}_{422}\dot{\mathrm{q}}_2^2 + \mathrm{h}_{433}\dot{\mathrm{q}}_3^2 + \mathrm{h}_{444}\dot{\mathrm{q}}_4^2 + \mathrm{h}_{412}\dot{\mathrm{q}}_1\dot{\mathrm{q}}_2 + \mathrm{h}_{413}\dot{\mathrm{q}}_1\dot{\mathrm{q}}_3 + h_{414}\dot{q}_1\dot{q}_4 + h_{423}\dot{q}_2\dot{q}_3 + h_{424}\dot{q}_2\dot{q}_4 + h_{434}\dot{q}_3\dot{q}_4 + C_4 \quad (9)$$

The coefficients C_i, D_{ij} h_{ijk} in Equations 6 to 9 are functions of both the joint variables and inertial parameters of the manipulator, and can be called "the dynamic coefficients of the manipulator". The physical meaning and functional properties of these three dynamic coefficients can be identified from the defining expression, Equation 3.

The gravity field is parallel to the z direction of the base coordinate

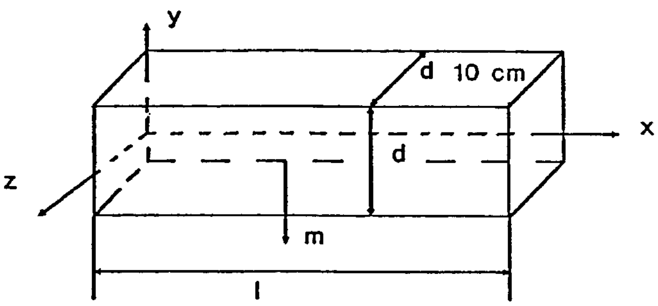

Fig. 2. Shape of Link

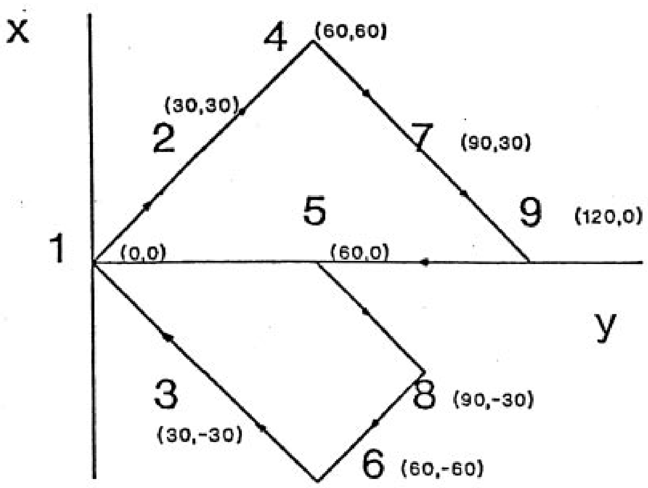

Fig. 3. The Path in The XY Plane

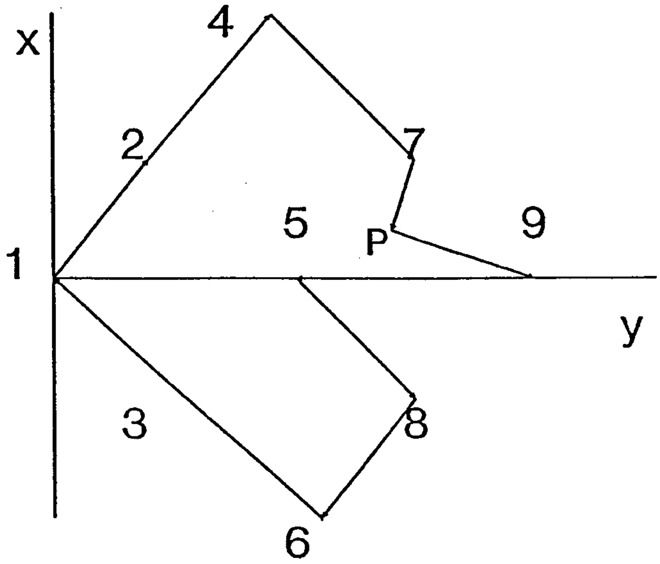

Fig. 4. The Path For Obstacle Avoidance

$$G = [0 \quad 0 \quad -g \quad 0] \quad (10)$$

where g is acceleration due to gravity. For the first four manipulator joints, the coefficients defined by Equation 3, are:

$$C_1 = -(m_1 GU_{11} r_1 + m_2 GU_{21} r_2 + m_3 GU_{31} r_3 + m_4 GU_{41} r_4) \quad (11)$$

$$C_2 = -(m_2 GU_{22} r_2 + m_3 GU_{32} r_3 + m_4 GU_{42} r_4 \quad (12)$$

$$C_3 = -(m_3 GU_{33} r_3 + m_4 GU_{43} 4_4) \quad (13)$$

$$C_4 = -(m_4 GU_{44} r_4) \quad (14)$$

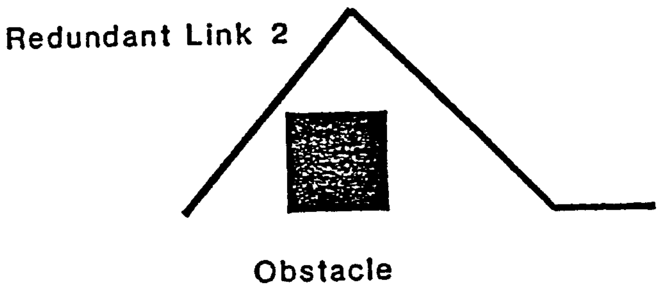

Fig. 5. Reaching Around an Obstacle With Redundant Manipulator

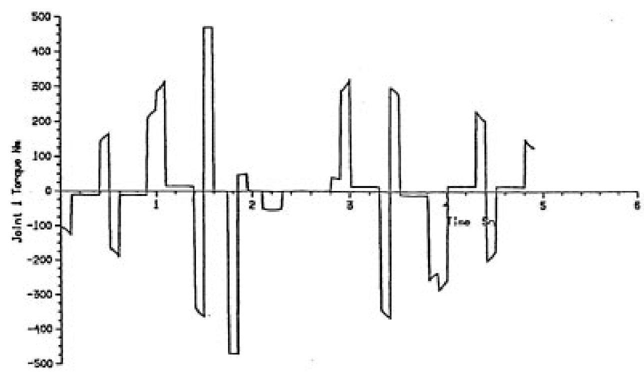

Fig. 6. Joint 1 Torque

https://doi.org/10.1017/S0263574798000617 Published online by Cambridge University Press

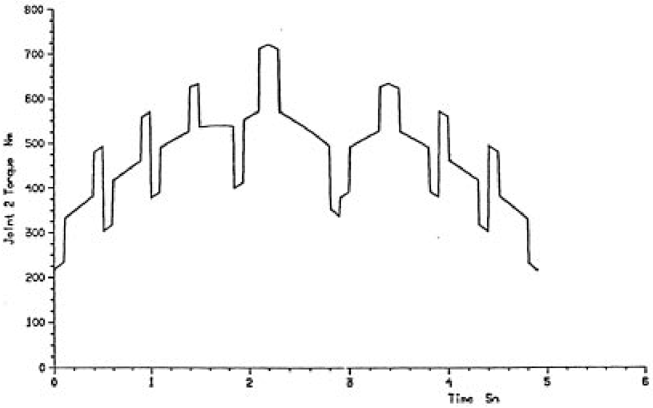

Fig. 7. Joint 2 Torque

2.1 *Acceleration Related Coefficients*

Due to the symmetry of the $D(q)$ matrix shown in Equation 4 only ten dynamic coefficients are evaluated, four diagonal and six off-diagonal coefficients. The dynamic coefficients D_{ii} relate the total inertia at joint 'i' to the acceleration of the same joint. The off-diagonal coefficients D_{ij} relate to the dynamic interaction at joint 'i' due to an acceleration at 'j'. From Equation 4 these are:-

$$
\begin{aligned}
&D_{11} = Tr(U_{11}J_1U_{11}^T) + Tr(U_{21}J_2U_{21}^T) + Tr(U_{31}J_3U_{31}^T)\\
&\qquad + Tr(U_{41}J_4U_{41}^T)\\
&D_{12}Tr(U_{22}J_2U_{21}^T) + Tr(U_{32}J_3U_{31}^T + Tr(U_{42}J_4U_{41}^T)\\
&D_{13} = +Tr(U_{33}J_3U_{31}^T) + Tr(U_{43}J_4U_{41}^T)\\
&D_{14} + Tr(U_{44}J_4U_{41}^T)\\
&D_{22} = Tr(U_{22}J_2U_{22}^T) + Tr(U_{32}J_3U_{32}^T) + Tr(U_{42}J_4U_{42}^T\\
&D_{23} = Tr(U_{33}J_3U_{32}^T) + Tr(U_{43}J_4U_{42}^T)\\
&D_{24} = Tr(U_{44}J_4U_{42}^T)\\
&D_{33} = Tr(U_{33}J_3U_{33}^T) + Tr(U_{43}J_4U_{43}^T)\\
&D_{33} = Tr(U_{44}J_4U_{43}^T)\\
&D_{44} = Tr(U_{44}J_4U_{44}^T) \qquad (15)
\end{aligned}
$$

3. DYNAMIC EQUATION FOR REDUNDANT MANIPULATOR

As mentioned in Section 2, dynamic coupling between motions of different joints exists only when links are moving relative to each other. For this reason, only the first four joints are of interest and of these, joint 2 is assumed to be locked for obstacle avoidance. Therefore, only joints 1, 3 and 4 will be discussed in this section.

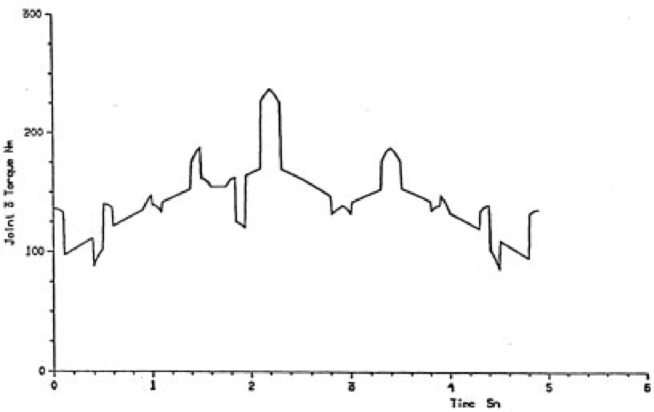

Fig. 8. Joint 3 Torque

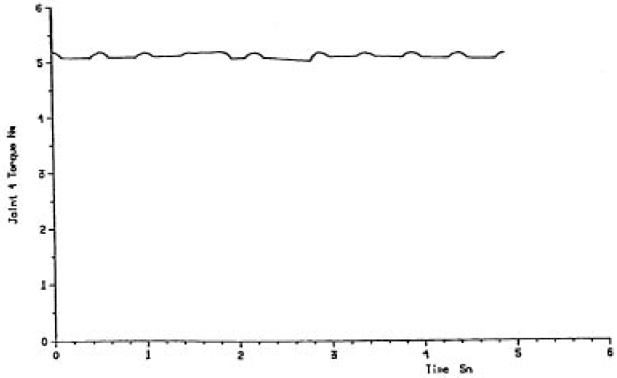

Fig. 9. Joint 4 Torque

To distinguish between the dynamic coefficients of the redundant and non-redundant manipulator the '*' symbol is introduced, ie C_i^*, D_i and h_{ijk}.

3.1 *Gravity terms*

In the evaluation of the gravity terms, the field of gravity is known to be parallel to the z direction of the base coordinate frame. The coefficients defined by Equation 4, are:-

$$C_1^* = -(m_1^* G U_{11}^* r_1 + m_3 G U_{31}^* r_3 + m_4 G U_{11}^* r_4) \qquad (16)$$

$$C_1^* = 0$$

$$C_3^* = -(m_3 G U_{33}^* r_3 + m_4 G U_{43}^* r_4) \qquad (17)$$

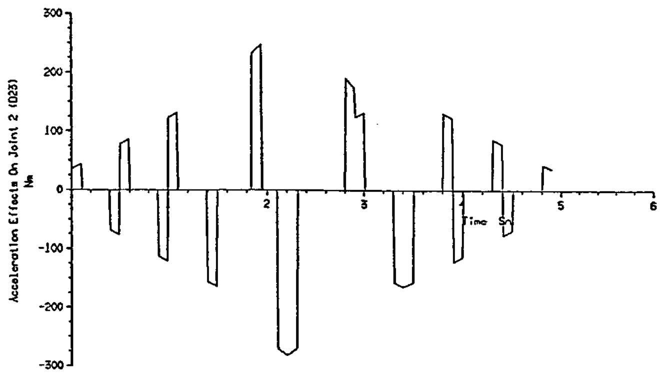

Fig. 10. Joint 5 Torque

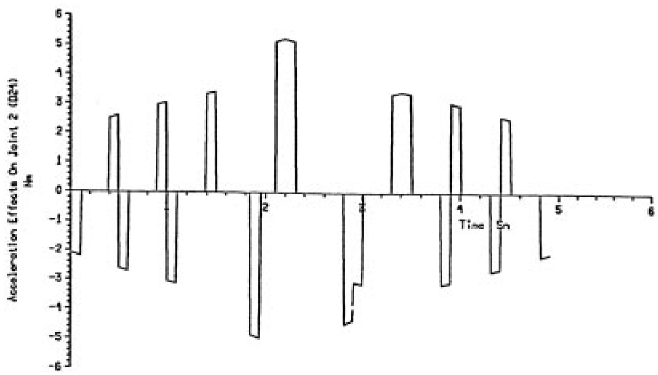

Fig. 11. D24 Relates Acceleration Torque at Joint 2

https://doi.org/10.1017/S0263574798000617 Published online by Cambridge University Press

$$C_3^* = \frac{1}{2} m_3 g l_3 c_3 + \frac{1}{2} m_3 g l_4 c_{44}$$

$$C_4^* = -(m_4 G U_{44}^* r_4)$$

$$C_4^* = \frac{1}{2} m_4 g l_4 c_{34} \tag{18}$$

It is apparent from an inspection of Figure 1, the axis of rotation of joint 1 is always parallel to the field of gravity, hence joint 1 will not experience a torque due to gravity.

This circumstance corresponds to zero values for the elements GU_{11}, GU_{12} and GU_{31} defined by Equation 16, since the third row terms U_{11}, U_{21} and U_{31} are all of zero value. Equation 17 gives the gravity term as a function of q_3 and q_4 incident at joint 3 and the gravity torque at joint 4 is a function of the joint angles q_3 and q_4.

3.2 Acceleration related dynamic coefficients

Due to the symmetry of the matrix, only six acceleration-related dynamic terms are evaluated for the model; three diagonal and three off-diagonal coefficients. The diagonal coefficients are

$$D_{11}^* = Tr(U_{11} J_1 U_{11}^T) + Tr(U_{21} J_2 U_{21}^T) + Tr(U_{31} J_3 U_{31}^T)$$
$$D_{22}^* = Tr(U_{22} J_2 U_{22}^T) + Tr(U_{32} J_3 U_{32}^T)$$
$$D_{33}^* = Tr(U_{33} J_3 U_{33}^T) \tag{19}$$

and the off-diagonal coefficients are

$$D_{12}^* = Tr(U_{22} J_2 U_{21}^T) + Tr(U_{32} J_3 U_{31}^T)$$
$$D_{13}^* = Tr(U_{33} J_3 U_{31}^T)$$
$$D_{23}^* = Tr(U_{33} J_3 J_{32}^T) \tag{20}$$

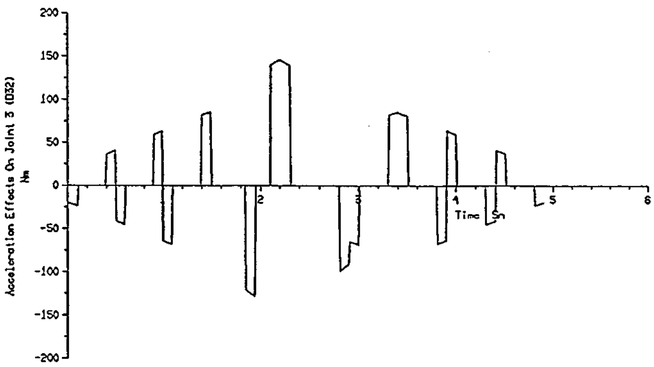

Fig. 12. D32 Relates Acceleration Torque at Joint 3

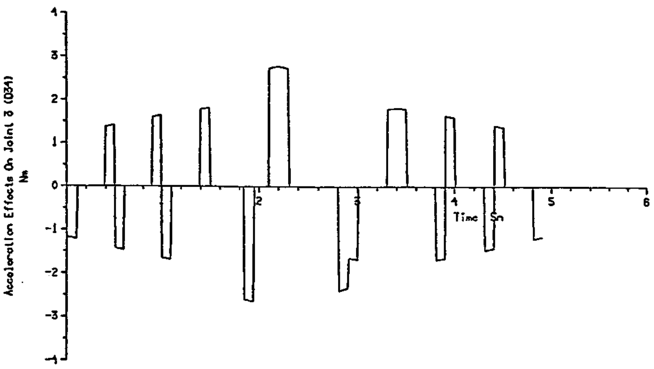

Fig. 13. D34 Relates Acceleration Torque at Joint 3

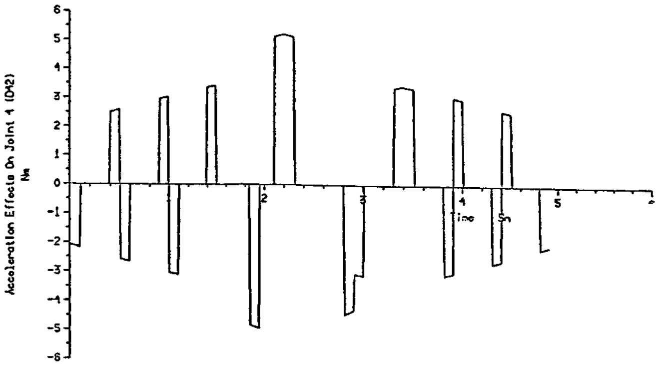

Fig. 14. D42 Relates Acceleration Torque at Joint 4

After some algebra and trigonometric manipulation the following expression can be derived from Equations 19 and 20

$$D_{11}^* = m_2 l_2^2 \left(\frac{1}{2} - c_2 + c_2^2 \right) + m_1 l_2^2 c_2^2 + \frac{1}{3} m_3 l_3^2 c_3^2 + m_2 l_2 l_3 c_2 c_3$$
$$+ m_3 l_2^2 c_2^2 + \frac{1}{3} m_4 l_4^2 c_{34}^2 + m_4 l_3 l_4 c_2 c_{34} + m_4 l_2 l_4 c_2 c_{34}$$
$$+ m_4 l_3^2 c_3^2 + m_4 l_2^3 c_2^2 \tag{21}$$

$$D_{22}^* = \frac{1}{3}(m_3 l_3^2 + m_4 l_4^2) + m_4 l_3 (l_4 c_4 + l_3) \tag{22}$$

$$D_{33}^* = \frac{1}{3} m_4 l_4^2 \tag{23}$$

$$D_{12}^* = 0 \tag{24}$$

$$D_{13}^* = 0 \tag{25}$$

$$D_{23}^* = m_4 l_4 \left(\frac{1}{3} l_4 + \frac{1}{2} l_3 c_4 \right) \tag{26}$$

3.3 Coriolis and centrifugal terms

The velocity related coefficients of the Coriolis and Centrifugal terms, are derived below for $i = 3$

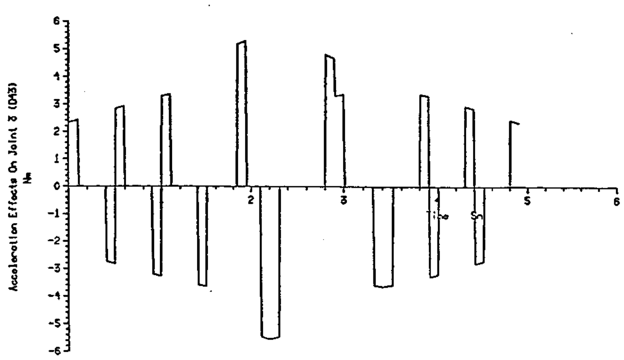

Fig. 15. D43 Relates Acceleration Torque at Joint 4

https://doi.org/10.1017/S0263574798000617 Published online by Cambridge University Press

$$h_1^* = h_{122}\dot{q}_1\dot{q}_2 + h_{121}\dot{q}_1\dot{q}_2 + h_{133}\dot{q}_1\dot{q}_3 + h_{131}\dot{q}_1\dot{q}_{33} \tag{27}$$

$$h_3^* = h_{311}\dot{q}_1^2 + h_{333}\dot{q}_3^2 + 2h_{334}\dot{q}_3\dot{q}_4 + h_{344}\dot{q}_4^2 \tag{28}$$

$$h_4^* = h_{411}\dot{q}_1^2 + h_{433}\dot{q}_3^2 \tag{29}$$

Finally, the Lagrange-Euler equations for the joints 1, 3 and 4, can be obtained:

$$T_1^* = D_{11}\ddot{q}_1 + D_{12}\ddot{q}_2 + D_{13}\ddot{q}_3 + 2h_{112}\dot{q}_1\dot{q}_2 + 2h_{113}\dot{q}_1\dot{q}_3 + C_1 \tag{30}$$

$$T_3^* = D_{31}\ddot{q}_1 + D_{33}\ddot{q}_3 + D_{34}\ddot{q}_4 + h_{311}\dot{q}_1^2 + h_{333}\dot{q}_3^2 + h_{344}\dot{q}_4^2 \; h_{334}\dot{q}_3\dot{q}_4 + C_3 \tag{31}$$

$$T_4^* = D_{41}\ddot{q}_1 + D_{42}\ddot{q}_2 + D_{44}\ddot{q}_4 + h_{411}\dot{q}_1^2 + h_{422}\dot{q}_2^2 + C_4 \tag{32}$$

The torque components acting at the different manipulator joints are essential parameters in a dynamic simulation and control system design study. The transient and steady state performance is dictated by how well these torque parameter values can be controlled, information being available to the engineer from a dynamic simulation.

4. MOMENT OF INERTIA

The evaluation of the inertia matrix elements is always a major problem facing the practitioner. The shape, size and material used in a link will dictate the actual value. Consider a link as shown in Figure 2 with the individual reference frame located at the centre and parallel to the sides of the link section, so that it is symmetrical with respect to the y and z axes. Equation 5 the terms, I_{xx}, I_{yy} and I_{zz} are the moments of inertia about the x_i, y_i, z_i axes, respectively, and I_{ij} ($i \neq j$) are the products of inertia. When two axes of a reference frame form a plane of symmetry for the mass of the body, the product of inertia terms in the matrix Equation 5 is zero.[3,6,7] The term J_i is the inertia matrix of link i about the ith coordinate frame and this can be written as:-

$$J_i = \begin{matrix} \frac{1}{3}m_i l_i^2 & 0 & 0 & -\frac{1}{2}m_i l_i \\ 0 & 0 & 0 & 0 \\ 0 & 0 & 0 & 0 \\ -\frac{1}{2}m_i l_i^2 & 0 & 0 & m_i \end{matrix} \tag{33}$$

The procedure for calculating the inertia matrix element of I_{ij} can be found in several textbooks,[8–10] where a detailed explanation is given.

5. RESULT OF COMPUTER SIMULATION

The dynamic analysis for the manipulator joint torques has been undertaken for two different cases using the computer program developed in both cases where the initial configurations of the manipulator are the same. The path followed in each case is different because of obstacles. In this work, the manipulator is assumed to move in the xy plane, as shown in Figure 3.[11] In Figure 4 the direct motion of the end-effector from point 7 to 9 will result in a collision

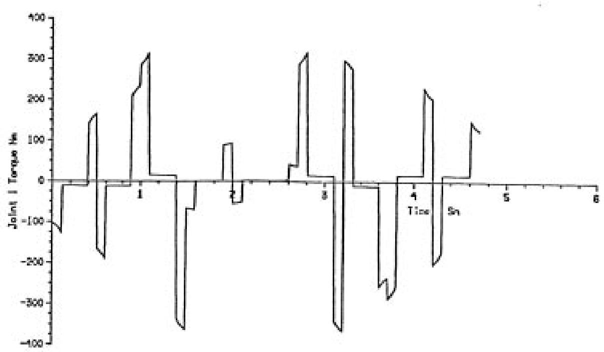

Fig. 16. Joint 1 Torque

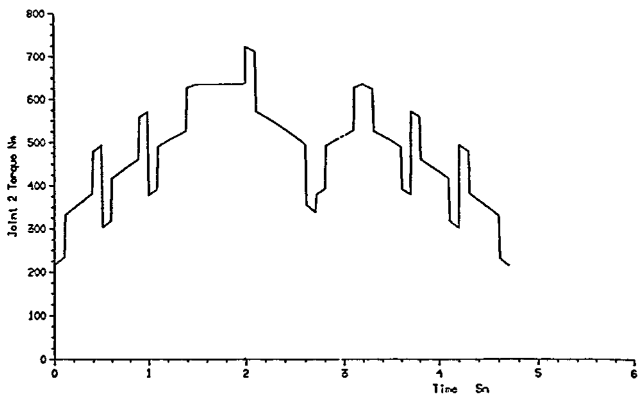

Fig. 17. Joint 2 Torque

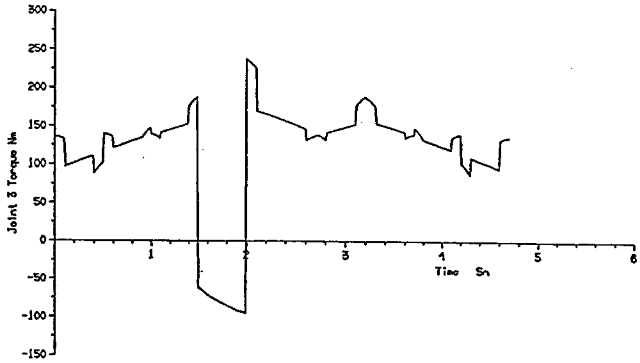

Fig. 18. Joint 3 Torque

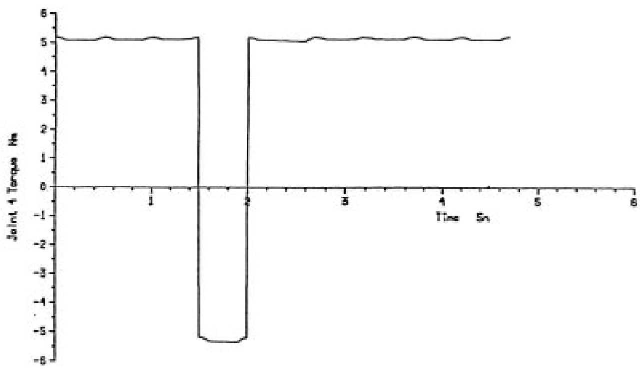

Fig. 19. Joint 4 Torque

https://doi.org/10.1017/S0263574798000617 Published online by Cambridge University Press

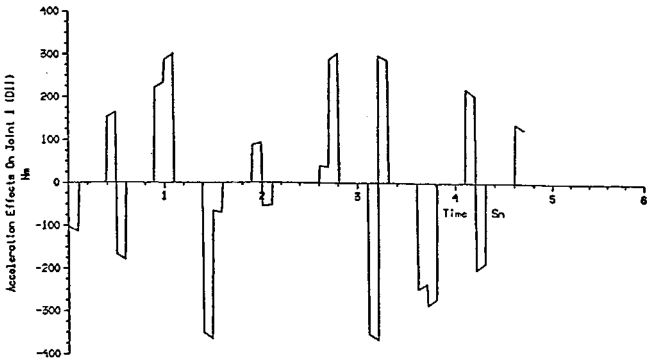

Fig. 20. D11 Relates Acceleration Torque at Joint 1

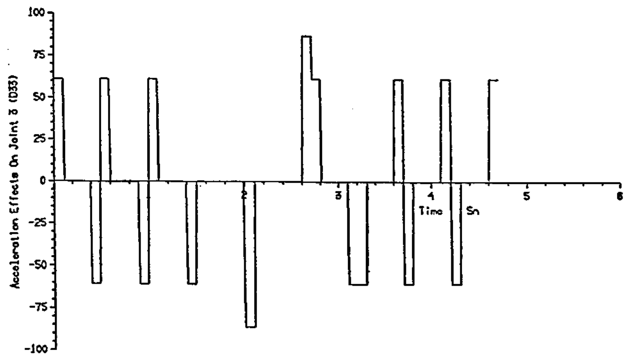

Fig. 22. D33 Relates Acceleration Torque at Joint 3

at link 2, as shown in Figure 5. There are two possible ways to avoid this collision. The first is to find a route which prevents link 2 from striking the object. A route can be found for the end-effector along the path 7-P-9 shown in Figure 4 to avoid a collision. The second is to lock joint 2 which will enable the end-effector to move directly from point 7 to point 9.

5.1 Case I (non-redundant configuration)

In this case, the path followed by the end-effector is identified in Figure 4. When the end-effector arrives at point 7, the route followed in this case will be 7-P-9. The results available from the dynamic simulation permit the required actuator torques to be predicted and these are shown in Figures 6 to 9 for the constraints imposed and the end-effector path chosen. The reaction torques occurring at other joints are given in Figures 10 to 15.

The simulation results show the impact of the motion of one joint on another and indicates the extent to which a joint controller must compensate for joint interactions. When designing a manipulator the following factors should be noted: that a significant amount of actuator power can be expended in overcoming gravitational force, leaving little energy for overcoming external factors; the lighter the material from which the links are constructed the lower the load on the actuators.

5.2 Case II (redundant configuration)

The manipulator's initial configuration remains the same as Case I but the path is that shown in Figure 3. When the end-effector reaches the point 7, link 2 is locked and remains so until point 9 is reached, at which point link 2 is released. For this situation the joint torque are given in Figures 16 to 19.

The acceleration-related coefficient $(D_{ij})_j$ values of which are not zero, are given in Figures 20 to 23 and the gravity forces are given in Figures 24 to 27.

The results of this dynamic simulation show that for most of the motion the gravity terms are larger than the inertia terms. The manipulator simulation presented can readily be extended to include a control system. This extended program would be available to study controller behaviour to ensure transient and steady state performance.

The evaluation of the joint torques based on the complete *L-E* equations of motion is complex and computationally expensive. As a result, approximations must be made when this model is incorporated into a real-time digital control loop. The simplifications that can be made, with confidence, are identifiable from results similar to those presented in this chapter. For instance, the extent to which a controller must compensate for joint interactions; that is, when can the off-diagonal elements of $D(q)$ be equated to zero? In what circumstances can the robot motion be considered to be slow and the whole of the $D(q)$ matrix neglected?

This operational information is readily available from the computer simulation developed in this project for use by the industrial practitioner.

6. DISCUSSION

The torque components acting at the different manipulator joints are essential parameters in deciding if specific tasks can be performed by the robots available. The dynamic

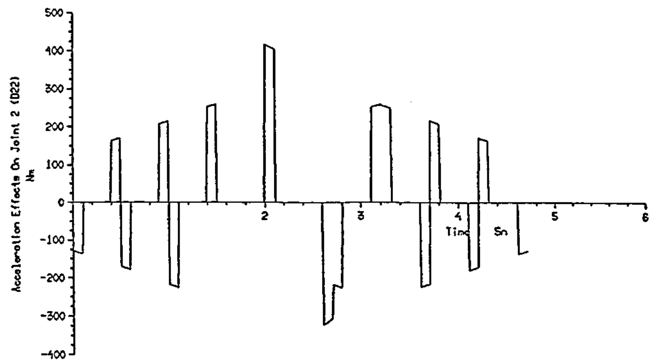

Fig. 21. D22 Relates Acceleration Torque at Joint 2

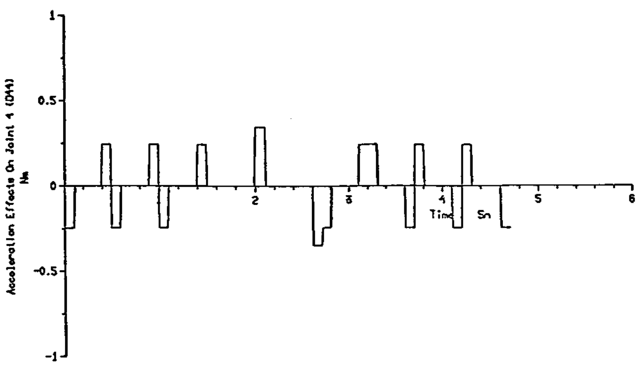

Fig. 23. D11 Relates Acceleration Torque at Joint 4

https://doi.org/10.1017/S0263574798000617 Published online by Cambridge University Press

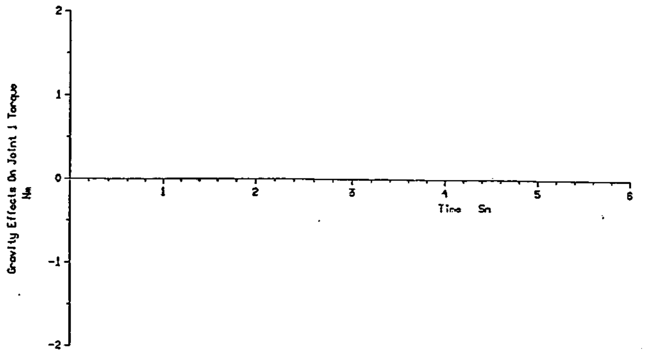

Fig. 24. Gravity Force at Joint 1

analysis software developed can be directly used by an industrial engineer to select a suitable actuators if modification of an existing robot is a cost-effective solution for a new application.

A number of design considerations arise from the result of the dynamic study. The further an object is from a joint and the larger its mass, the greater will be the resulting

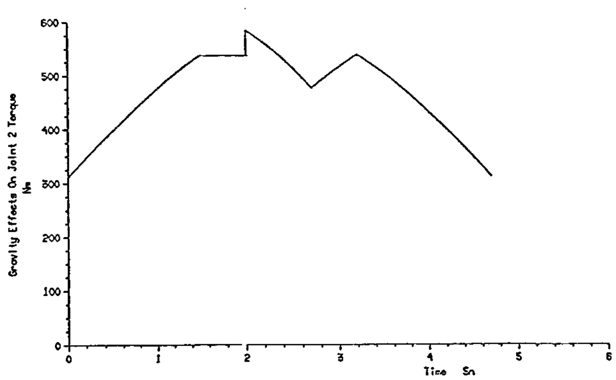

Fig. 25. Gravity Force at Joint 2

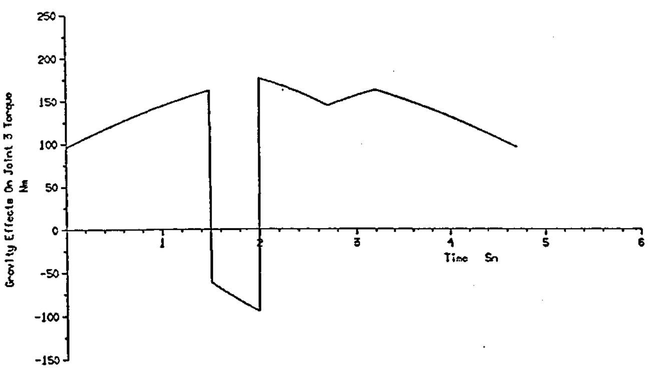

Fig. 26. Gravity Force at Joint 3

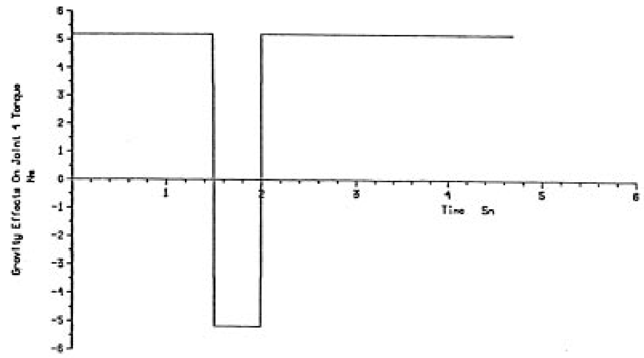

Fig. 27. Gravity Force at Joint 4

inertial torques. Such torques are transferred inwards towards the base of the robot resulting in increased joint torques. Reducing the mass of a link and shifting this mass towards the base by relocating the actuators at the base, will reduce the torques required to overcome inertia.

A less complex robot link design can lead to a diagonal inertia tensor, eliminating the products of inertia, and this will considerably reduce the complexity of the dynamic equations. A second reason for using physically simple-shaped links is that they are more readily modelled and hence, the estimates of the moments of inertia will be more accurate. Link stiffness is important and flexibility will cause errors in a following trajectory. Modelling of flexible link structures is a subject of continuing research and beyond the scope of this project.

References

1. J.H. Ginsberg, *Advanced Engineering Dynamics* (Harper Row Publisher, New York, 1988).
2. R.P. Paul, *Robot Manipulators: Mathematics, Programming and Control* (MIT Press, Cambridge, Mass., 1982).
3. K.S. Fu, R.C. Ganzales and C.S.G. Lee, *Robotic Control Sensing, Vision and Intelligence* (McGraw-Hill, New York, 1987).
4. R.J. Schilling *Fundamentals of Robotics Analysis and Control* (Prentice-Hall, New York, 1990).
5. A.K. Bejczy, "Robot Arm Dynamics and Control", *Technical Memorandum 33–669* (Jet Propulsion Lab, California, 1974).
6. A.J. Koivo, *Fundamentals for Control of Robotic Manipulators* (John Wiley and Sons, 1989).
7. G.N. Saridis, *Advances in Automation and Robotics* (JAI Press, 1985).
8. K.A. Stroud, *Engineering Mathematics* (Macmillan, London, 1991).
9. F.P. Beer and E.R. Johnston, *Mechanics for Engineers* (McGraw-Hill, New York, 1987).
10. M.W. Spong and M. Vidyasagar, *Robot Dynamics Control* (John Wiley and Sons, New York, 1984).
11. M. Eroglu and K.F. Gill "Trajectory plannig using artificial intelligence", *Proc. Inst. Mech. Engrs.* **207**, 193–198 (1993).